Aircraft Position Estimation during Intermittent Loss-of-Signal using Regression/EKF-Based State Estimation

1st Michael Dacus
Department of Aeronautics and Astronautics
Stanford University
Stanford, CA, USA
mwdacus@stanford.edu, ORCID: 0000-0002-4363-4981

***Abstract*—The ability to estimate aircraft position and velocity is vital for safe and effective air traffic operations and management. With the emergence of the Automatic Dependent Surveillance-Broadcast (ADS-B) network, aircraft are now capable of sending GNSS positioning and operational data to ground stations to be used by regional air traffic controllers. On rare (but possible) situations, aircraft may lose ADS-B signal reception due to a variety of reasons, so it is important to formally derive a position solution of the aircraft during ADS-B reception loss.**

This paper seeks to use historical crowdsourced ADS-B data to implement variations of the Extended Kalman Filter (EKF) during intermittent loss of ADS-B reception. Crowdsourced data is retrieved from OpenSky Network, a client-based application that receives air traffic data from a network of ADS-B receivers around the globe. This newly estimated state is then compared to a real world flight test case scenario from Edwards Air Force Base (AFB) in September 2019, where several test flights from a C-12J Huron were conducted. By comparing this estimated state with the onboard receiver data, results have indicated that using ADS-B only does not perform as well as ADS-B with control input information from UHARS, but manages to track the aircraft for prolonged trajectories.

***Index Terms*—ADS-B, EKF, GPS/GNSS, Interference**

I. Introduction

The Automatic Dependent Surveillance-Broadcast (ADS-B) is a series of receiver ground stations (primarily within the United States and Europe (EU)) that serve as a network to collect local GPS positioning, velocity and operational messages (transmitted via 1090 MHz frequency) from aircraft flying within its local airspace [1]. The ADS-B network has had an increasing role in air traffic and management operations within the National Airspace System (NAS) over the past decade, and with requirements from both the Federal Aviation Administration (FAA: United States) and the European Union Aviation Safety Administration (EASA: EU) for all aircraft to have installed ADS-B Out equipment by 2020, ADS-B has already transitioned into a fully operational and available status across CONUS and Western Europe.

ADS-B provides several unique advantages over traditional radar-based methods. The primary benefit is that ADS-B provides aircraft positioning updates every 0.5 seconds, whereas radar takes 5-12 seconds to reestablish an aircraft's location. Other unique features include real-time weather and traffic updates, allowing for improved situation awareness and decision-making by both pilots and air traffic controllers. There are also disadvantages, specifically the possibility of losing reception to local ADS-B ground stations, resulting in gaps in the observed flight path trajectory. ADS-B reception loss can be due to a variety of reasons, whether it is from physical signal blockage, beyond Line-Of-Sight (LOS) to a physical ADS-B ground station, or various forms interference and jamming. Some research (as noted in Section II-A) use ADS-B data to determine whether aircraft are affected by regional jamming sources (GNSS or other RFI), whereas other fields (noted in Section II-B) use the data to predict flight path trajectories. Regardless of the end purpose, State Estimation with ADS-B is vital for accurate and reasonable prediction of air traffic, and how ADS-B affects air travel.

This paper seeks to interpolate existing aircraft trajectories (using a localized regression approach) in combination with Extended Kalman Filtering (EKF) techniques during intermittent loss of ADS-B Reception, with the efforts to determine an aircraft's estimated state. The proposed EKF approaches are then applied to a real world flight test data from a C-12J Huron from the 586th Flight Test Squadron from Edwards Air Force Base (AFB), California. The data recorded from the flight test is called UHARS (Ultra High Accuracy Accuracy System), a data source recorded by a series onboard sensors (IMU's, GPS, and aircraft instrumentation) that results in a high-accuracy positioning solution for the aircraft. As it relates to the proposed EKFs and the ADS-B data, the UHARS data from the flight test will be considered as the "true state." ADS-B data (which is treated as observation data) is gathered from the OpenSky Network, an open-source, research-based ADS-B receiver network that gathers aircraft positioning from commercial and private aircraft around the world. [2]

Section II discusses various applications of ADS-B data in both State Estimation and IDL fields. Section III discusses processing techniques for both the UHARS and ADS-B data. Section IV discusses the two EKF approaches to the state estimation problem, and Section V shows the estimated state results for two portions of the flight test.

II. Literature Review

In order to fully understand the nature of potential intermittent loss of ADS-B reception, it is important to provide a review on the state of both GNSS interference detection (using ADS-B) and state estimation research fields. Understanding how ADS-B data is used to detect GNSS interference sources may be helpful in learning how aircraft lose ADS-B reception during flight. Equally as important, a literature review of the state estimation field could provide an idea behind the possible research gaps into incorporating ADS-B in various filtering methods, and how the field overall might be improved.

A. Research involving GNSS Interference Detection and Localization (IDL)

Currently in the field, many researchers that use ADS-B for IDL detection primarily rely on Machine Learning (ML) based methods. Darabseh et al. [3] constructs various probability distributions for anomaly detection using the Navigational Accuracy Category, Position (NACp) values from OpenSky receiver data. Liu et. al [4] implements a Neural Network algorithm for detecting interference by predicting the Navigational Integrity Category (NIC) from a latitude-longitude-altitude (LLA) positioning of aircraft over a period of time. Liu et. al [5] also calculates the relative position of a GNSS jammer by reformulating the problem as a convex optimization problem.

Based on the event analyzed in that paper (Hayward Executive Airport), ADS-B data showed that aircraft that lost ADS-B signal re-established reception after passing over the jammer location, which ranged from 30 seconds to 1.5 minutes, which will be useful in the proposed data interpolation method. Other papers noted a similar duration of signal loss, and will continued to be assessed in reviewing other papers.

B. Specific Research on Aircraft Estimation and Prediction Techniques

Currently in the field, aircraft state estimation is formulated either as a data-driven model, or Discrete Time Model using defined aircraft dynamics. For data driven models, several papers implement a series of deep learning and interpolation techniques. Adesina et al. [6] explores using this metadata with Deep Neural Networks (DNN) and Support Vector Regressors (SVRs), and found them to perform far better than traditional multilateration (MLAT). Strohmeier et al. [7] uses a k-Nearest Neighbor (k-NN) approach to aircraft localization by training historical aircraft trajectories, and their results show a smaller aircraft position error bound. Ayhan et al. [8] formulates the problem as a Hidden Markov Model (HMM) and uses weather observations and real time positioning data to predict future aircraft trajectories. Finally, Xu et. al [9] and Zeng et. al [10] incorporate variations of LSTM models on trained ADS-B data to predict future aircraft trajectories within regional airspace.

For papers that implement some form of Discrete Time Model, the Kalman Filter (KF) (or variations thereof) is the most widely used. Xi et. al [11] uses a KF for conventional 6D aircraft state estimation. Jing et. al [12] uses an Unscented Kalman Filter (UKF) to estimate the state of jet aircraft while accommodating external effects, such as wind shear and potential high turbulence. By accounting for these effects, the UKF relies on additional aerodynamic parameters as well as nonlinear feedback control. And finally, Bauer et al. [13] implements an EKF on data collected from NASA's X-29, a retired experimental flight test aircraft. While the latter two papers did not incorporate ADS-B data into their aircraft dynamics and/or measurement model equations, it could be beneficial in merging these concepts with ADS-B data sources.

Additional papers (outside the ADS-B community, pertaining to aircraft state estimation) rely on a mixture between either discrete dynamics and data driven models, as well as a number of data sources, including onboard GPS receiver data, analog aircraft instrumentation, radar, and other ground-based measuring equipment.

III. Data Processing and Interpolation

A. UHARS Data

The UHARS data collected during the flight test does not require much data filtering prior to implementation into the proposed EKF. Beyond sorting data into respective state variables, the time is converted from GPS Time (originally in Leap Seconds) to Universal Coordinated Time (UTC) in order to match with the corresponding ADS-B Data. The latitude, longitude, an altitude data is converted to an East-North-Up (ENU) coordinate system, with a local origin established at the first available timestamp.

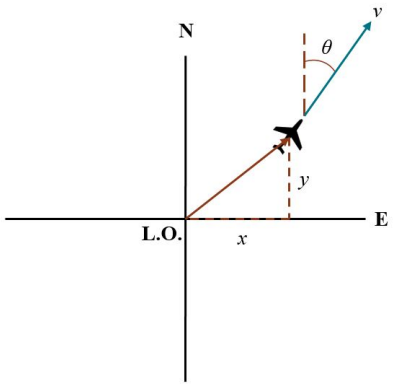

Fig. 1. Localized East-North-Up (ENU) Coordinate System Setup with Up direction coming out of page (altitude z and vertical rate $\dot{z}$ not shown)

B. ADS-B Data

1) Data Processing: After the ADS-B data is retrieved from OpenSky, it must be pre-processed prior to usage within the EKF filter formulations. First, duplicate ADS-B messages (messages with the same timestamp and position fix) are removed from the dataset, in addition to inconsistent receiver time clocks (the timestamp associated to when a particular ADS-B message is received at a ground station). An inconsistent receiver clock is similar to an incorrect position fix, so the corresponding ADS-B mesages should be removed. Messages with incomplete information are also removed. In addition,

ADS-B messages with faulty positioning messages (due to possible reasons discussed in Section I) must be removed, in order for the localized interpolation to provide a reasonable flight path trajectory. To detect outliers, a similar method is similar to [14] where the relative error between a smoothing function (such as moving average smoothing function) and the data point is determined. From there, the outliers are removed if they are beyond 1.5 times the interquartile range (IQR) of the associated relative error.

2) Flight Path Interpolation: With the faulty ADS-B messages removed from the dataset, gaps in the ADS-B message can be determined. While there are many approaches to interpolating the flight path (both local or global), this project uses `geoTrajectory`, a MATLAB System Object that uses both positioning (in Geodetic coordinates) and velocity to reconstruct missing flight paths. This interpolation method is applied to ADS-B data with gaps between 15-60 seconds in reception loss. This interval was determined based on the existing literature as well as the assumption that a basic flight maneuver of an aircraft (straight-and-level, ascent, descent, and turning) can be performed within this timeframe; any combination of these flight maneuvers would result in a wider variety of trajectories, and thus a larger uncertainty for state estimation purposes.

IV. State Estimation Methodologies

With the data (both ADS-B and UHARS) processed and synchronized, an EKF can implemented to estimate the state of the aircraft. It is important to note that an EKF was chosen mainly due to the understanding that aircraft exhibit nonlinear dynamics. In this project, two variations of the EKF derived based on separate series of assumptions and observability of the dataset. Method 1 (derived in Section IV-A) assumes that no flight control information is given, whereas Method 2 (derived in Section IV-B) uses UHARS ground speed, course heading and vertical rate as control input values at each timestep. Both formulations do accommodate 2 bias terms (ADS-B clock offset bias and barometric altitude bias), and are discussed at greater length in Section IV-1 and IV-2.

1) Barometric Altitude Measurement Bias: In air traffic management, pilots and controllers alike rely on barometric altitude, which is determined by the barometric pressure of a certain area of airspace and the aircraft's static system for altitude reporting purposes. ADS-B primarily reports the barometric altitude value versus the GPS acquired altitude positioning solution. Based on data observation (as it can be noticed in Figures 2(b) and 5(b)), there is a fairly constant offset between the GPS and barometric altitude ($\approx$ 200 meters), and this offset can be combined into the state vector for estimation purposes.

2) ADS-B Clock Delay Bias: Another bias term that needs to be incorporated into the state vector is the ADS-B clock delay. For the ADS-B data, the timestamp associated with a particular positioning solution is the time the local ADS-B ground station received that ADS-B message, and not the time the aircraft was at that specified positioning coordinates. Therefore, once the data is processed, interpolated and synchronized (in this case, with the UHARS data), the ADS-B reported position will still be at some timed offset, which can be noticed in Figures 2(a) and 5(a); in both figures, the reported ADS-B position (green marker) is usually behind the UHARS positioning solution (red marker).

This bias term also serves as a "lumped" parameter for other undetermined error sources, including improper time synchronization with other ADS-B receivers, and general noise when the timestamp is generated.

A. Method 1: ADS-B Observable Only EKF

In the first formulation of the EKF, the main assumption incorporated - particularly in the definition of the state vector - is that there is no information regarding the control input of the aircraft. Therefore, the estimated state is an 8 dimensional vector (3 position, 3 velocity, and 2 bias) terms, as noted below:

$$\vec{x}_t = \begin{bmatrix} x & y & z & v & \theta & \dot{z} & \alpha_z & \beta_t \end{bmatrix}_t^T \tag{1}$$

where (x,y and z) are the position state variable (in ENU frame), v is the ground speed, θ is the course heading, and $\dot{z}$ is the vertical speed. The bias terms (α_z and β_t) are the Barometric Altitude Measurement and ADS-B Clock Delay bias terms. Since control input is unknown, the dynamics model is only dependent on the state vector with some assumed Gaussian White Noise $w_t \sim \mathcal{N}(0, Q)$

$$\vec{x}_{t+1} = f(\vec{x}_t) + w_t \tag{2}$$

where $f(\vec{x}_t)$ is the first-order discrete time dynamics model and Q is process noise covariance. The first-order discrete time dynamics model for an aircraft moving in 3D space is shown below:

$$\begin{aligned} x_{t+1} &= x_t + (\Delta t + \beta_t)\, v_t \sin(\theta_t) \\ y_{t+1} &= y_t + (\Delta t + \beta_t)\, v_t \cos(\theta_t) \\ z_{t+1} &= z_t + (\Delta t + \beta_t)\, \dot{z} \\ \{v_{t+1}, \theta_{t+1}, \dot{z}_{t+1}, \alpha_{z,t+1}, \beta_{t+1}\} &= \{v_t, \theta_t, \dot{z}_t, \alpha_{z,t}, \beta_t\} \end{aligned} \tag{3}$$

where the ground speed, course heading (the angle that is makes with the +y axis), vertical speed, and the bias terms are predicted using the previous time step state values. For the measurement model, a six-dimensional model (3 position, 3 velocity) is used, which can be shown below:

$$\begin{aligned} \vec{y}_t &= g(\vec{x}_t) + v_t, \text{ where,} \\ g(\vec{x}_t) &= \begin{bmatrix} x & y & z + \alpha_z & v & \theta & \dot{z} \end{bmatrix}^T \end{aligned} \tag{4}$$

where $v_t \sim \mathcal{N}(0, R)$. Notice that the barometric altitude measurement bias is incorporated into the altitude value.

With the dynamics and measurement models determined, dynamics Jacobian A_t and measurement Jacobian C_t are fairly straightforward derivations, and are shown along with the implemented EKF equations in Appendix VI-B.

It should also be noted that the process and measurement noise (Q and R respectively) were formulated for nominal conditions (i.e. relatively low turbulence and normal (NIC=9)

accuracy)). While the process noise can be tuned to meet "low turbulence conditions," for the purposes of this project, $Q = \Delta t \texttt{diag}([20\ 20\ 20\ 10\ 1\ 10\ 0\ 1])$ so that position state variables includes some position turbulence (20 [m]), while velocity and bias terms remained relatively low. For process noise, $R = \texttt{diag}([100\ 100\ 100\ 10\ 10\ 10])$, which is equivalent to a 95% containment radius of NIC=9. Greater discussion of the NIC value can be found in [5].

B. Method 2: ADS-B with UHARS Control Input Data

The formulation for the EKF in Method 2 follows a similar approach to Method 1, with the exception that control input of the aircraft is known, which is defined as:

$$u_t = \begin{bmatrix} v & \theta & \dot{z} \end{bmatrix}_t^T \tag{5}$$

where v is the ground speed, θ is the course heading, and $\dot{z}$ is the vertical velocity. Given the special circumstances of this problem, these control input values come from the provided UHARS dataset. Because of the added control input, the state vector is reduced to 5 dimensions (3 position and 2 bias terms), which is shown below:

$$\vec{x}_t = \begin{bmatrix} x & y & z & \alpha_z & \beta_t \end{bmatrix}_t^T \tag{6}$$

As a result, the dynamics model is in terms of the state and the control (still implementing a first order discrete time model), which is as shown below:

$$\begin{aligned} \vec{x}_{t+1} &= f(\vec{x}_t, u_t) + w_t \text{ where,} \\ x_{t+1} &= x_t + (\Delta t + \beta_t) u_{t,v} \sin(u_{t,\theta}) \\ y_{t+1} &= y_t + (\Delta t + \beta_t) u_{t,v} \cos(u_{t,\theta}) \\ z_{t+1} &= z_t + (\Delta t + \beta t) u_{t,\dot{z}} \\ \{\alpha_{z,t+1}, \beta_{t+1}\} &= \{\alpha_{z,t}, \beta_t\} \end{aligned} \tag{7}$$

where $u_{t,v}, u_{t,\theta}$,and $u_{t,\dot{z}}$ are from control input (Eq. 5).

Finally the measurement model is a three-dimensional vector (position only) since the velocity-related information is already known. The measurement model can be formulated as follows:

$$\begin{aligned} \vec{y}_t &= g(\vec{x}_t) + v_t \text{ where,} \\ g(\vec{x}_t) &= \begin{bmatrix} x & y & z + \alpha_z \end{bmatrix}_t^T \end{aligned} \tag{8}$$

The barometric altitude measurement bias is also incorporated in altitude, similar to Method 1's measurement model.

With the dynamics and measurement model, the dynamic and measurement Jacobians A_t and C_t can be formulated, which are shown along with the EKF equations in Appendix VI-C.

Similar to the justification of the process and measurment noise with Method 1, $Q = \Delta t \texttt{diag}([20\ 20\ 0\ 1])$ and $R = \texttt{diag}([100\ 100\ 100])$.

V. Results and Discussion

The following results of the estimated aircraft state are from two portions of the Edwards Flight Test Data, one of which occurred on September 11th, and the other on September 17th, 2019. Both events included a series of small gaps in flight data that were filled using the stated techniques. Both events also include a latitude-longitude view of each maneuver, as well as altitude change along the flight, and the relative error between the UHARS positioning solution and the estimated state of the aircraft, using both Method 1 and Method 2.

A. Portion of September 11, 2019 Flight

For the given portion of the September 11, 2019 flight, the flight test aircraft is heading eastbound and performs 2 360-degree counterclockwise clearing turns, resulting in an westbound course heading. Figures 2(a) and 2(b) show the aircraft trajectory (both observed ADS-B and UHARS true state) along with the estimated EKF trajectories approaches.

Figures 3 and 4 show the Relative Error (in ENU Coordinate Frame) of the estimated EKF positions (to the UHARS true state) for both Methods 1 and 2:

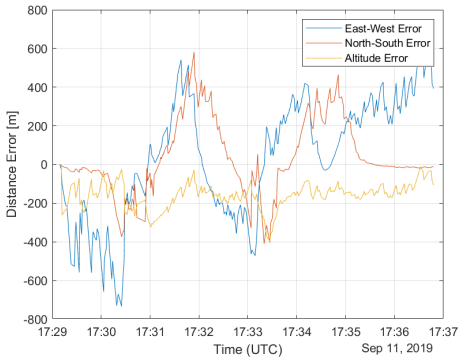

Fig. 3. Relative Error of ADS-B Only EKF Solution (Method 1) during Sept. 11, 2019 Flight

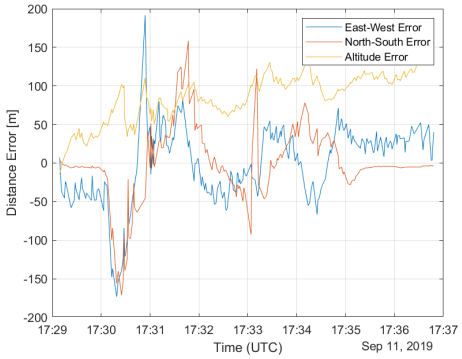

Fig. 4. Relative Error of ADS-B with UHARS Control Input (Method 2) during September 11, 2019 flight

Based on these figures, Method 1 seems to results in higher estimated uncertainty, which is expected given the fact that the control input is unknown. Among the relative errors, the altitude seem to have least overall error, which is desired since the EKF accounts for barometric altitude measurement bias. The areas of interpolated ADS-B data (around 17:31-17:32 UTC) noticed the highest relative error, which was also expected since they are not "true" observation data, but rather predicted observation measurements based on the overall trajectory of the flight path.

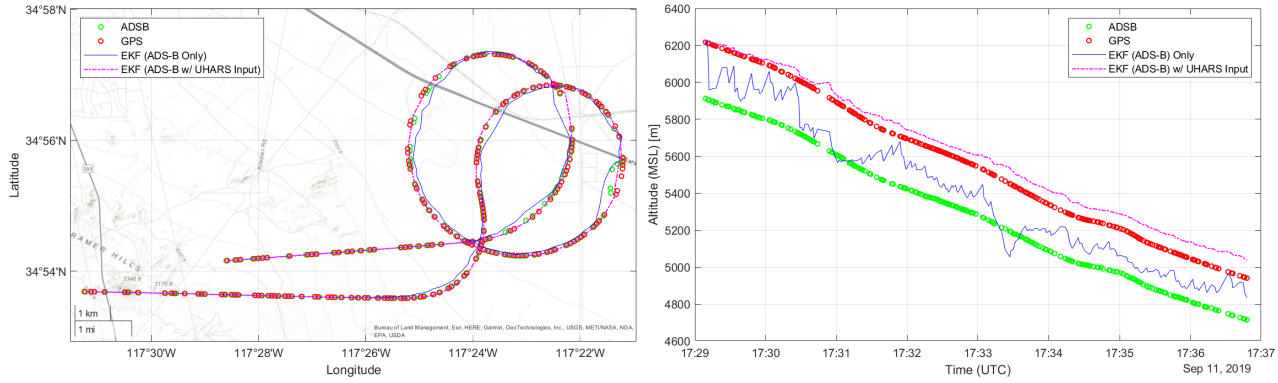

(a) (b)

Fig. 2. Portion of C-12J Flight Path (Topographic: Figure 2(a), Altitude: Figure 2(b)) near Edwards AFB on September 11, 2019

Full reliance on the ADS-B with no observability of aircraft input information - which is the most realistic scenario - will not perform as well Method 2, which, as mentioned before, incorporates the velocity data (from UHARS) as the control input. Figure 4 confirms this intuition as the relative error (for any dimension) does not exceed ± 150 meters, whereas Method 1 relative error can reach at most 600 meters, which could be undesirable in congested airspace where high accuracy state estimation is needed.

Besides observing the relative error, comparing the performance of the filters using Figure 2(b) also confirms the previously stated intuition. In the Figure, the EKF with incorporated UHARS velocity data as the control input (Method 2) aligned closer with the dynamics of the true state than Method 1, which experiences more as noisy data. However, Method 1's altitude is evenly split between with observed ADS-B data and the true state, indicating that barometric altitude measurement bias is active in some sense of addressing the noticeable offset with geometric altitude.

B. Portion of September 17, 2019 Flight

For the given portion of the September 17, 2019 flight, the flight test aircraft performs a slow 90-degree left turn from north to west, over a period of 2 minutes. The data that was interpolated was during the aircraft turn, which had no ADS-B information (for a period of approximately 20 seconds), possibly due to the aircraft banking. The latitude/longitude and altitude performance of both Method 1 and Method 2 are shown in Figure 5(a) and 5(b).

Similar to the Sept. 11 Flight, Figures 3 and 4 show the Relative Error (in ENU Coordinate Frame) of the estimated EKF positions for both Methods 1 and 2:

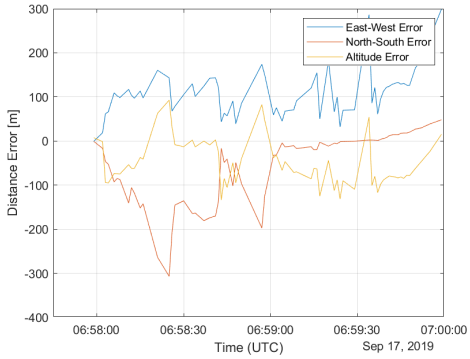

Fig. 6. Relative Error of ADS-B Only EKF Solution (Method 1) during Sept. 17, 2019 Flight

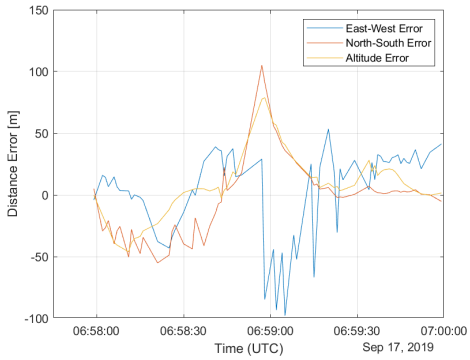

Fig. 7. Relative Error of ADS-B with UHARS Control Input (Method 2) during September 17, 2019 flight

A similar experience to that of the previous flight is shared with this flight. The Relative Error of Method 1 experiences more rapid fluctuations in the data ($\pm$ 200 meters) than the Relative Error of Method 2, which manages to remain bounded for the majority of the turn with $\pm$ 100 meters. Both however experience an increase in error during the loss of ADS-B reception (around 6:59 UTC) as noted by the sharp spikes, but they managed to reconverge towards to the true state.

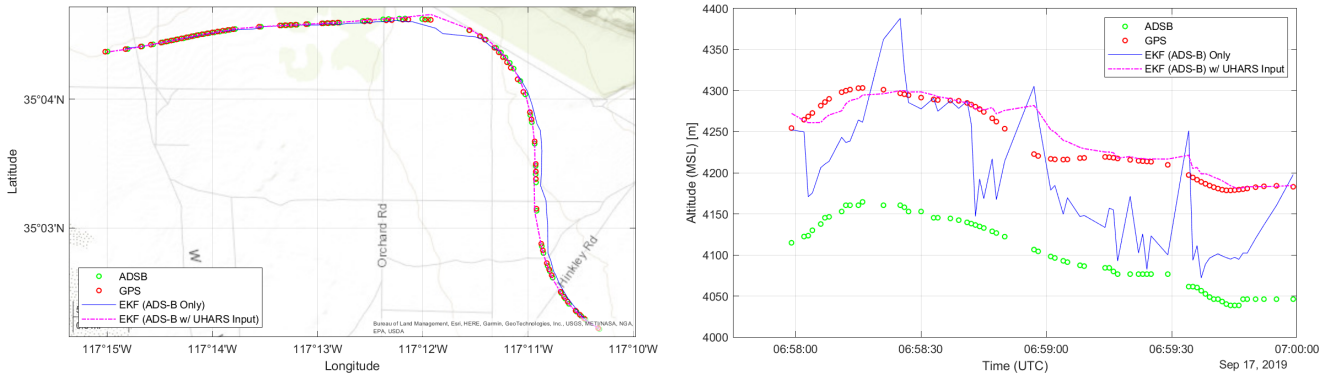

(a) (b)

Fig. 5. Portion of C-12J Flight Path (Topographic: Figure 5(a), Altitude: Figure 5(b)) near Edwards AFB on September 17, 2019

VI. Conclusion

This project implemented a series of EKF approaches (in combination with some preprocessing and data interpolation techniques) to predict an aircraft's estimated state. Method 1, while more realistic with regards to data acquisition, performed overall less accurate that Method 2, which incorporated high precision control input information from UHARS, a data source collected from a series of flight tests at Edwards AFB.

Both Methods ultimately represent a common problem revealed in state estimation theory and its practical application: the amount of observable data given based on the nature of the problem. While air traffic controllers and other ground operators receive a series of measurements (in the form of ADS-B) indicating the location of aircraft within a state space, they however don't receive all the information that could be beneficial to state estimation, in this case the pilot's control input. If however, the state estimation problem was formulated with respect to a "pilot" (UHARS), then having the control input would be known, and thus would allow for a more accurate positioning solution.

Future work will be mainly focused on improving the data preprocessing methods prior to EKF implementation. While this project used a localized interpolation approach (such as `geoTrajectory`), future versions will interpolate using a trained model from from historical flight paths (similar to [9] and [10]). This data driven approach could be used not only in predicting the flight path trajectory, but also determining whether existing ADS-B is reliable or faulty due to localized GNSS interference sources or regional RFI.

Acknowledgment

This paper is performed in conjunction with the author's ongoing work in Stanford's GPS Lab. The author would like to acknowledge and thank Dr. Todd Walter and Dr. Sherman Lo for their guidance on this project. The author would also like to thank the 586th Flight Test Squadron from Holloman AFB, NM for conducting the original flight test, and the collecting UHARS data.

References

[1] . C. 91.22, *Automatic Dependent Surveillance-Broadcast (ADS-B) Out equipment performance requirements*, 2013.

[2] M. Schäfer, M. Strohmeier, V. Lenders, I. Martinovic, and M. Wilhelm, "Bringing up opensky: A large-scale ads-b sensor network for research," in *IPSN-14 Proceedings of the 13th International Symposium on Information Processing in Sensor Networks*, 2014, pp. 83–94.

[3] A. Darabseh, E. Bitsikas, and B. Tedongmo, "Detecting gps jamming incidents in opensky data," *Proceedings of the 7th OpenSky Workshop 2019*, vol. 67, pp. 97–108, April 2014.

[4] Z. Liu, S. Lo, and T. Walter, "Gnss interference detection using machine learning algorithms on ads-b data," in *Proceedings of the 34th International Technical Meeting of the Satellite Division of The Institute of Navigation (ION GNSS+ 2021)*, 2021, pp. 4305–4315.

[5] ——, "Gnss interference characterization and localization using opensky ads-b data," *Proceedings*, vol. 59, no. 1, 2020. [Online]. Available: https://www.mdpi.com/2504-3900/59/1/10

[6] D. Adesina, O. Adagunodo, X. Dong, and L. Qian, "Aircraft location prediction using deep learning," in *MILCOM 2019 - 2019 IEEE Military Communications Conference (MILCOM)*, 2019, pp. 127–132.

[7] M. Strohmeier, I. Martinovic, and V. Lenders, "A k-nn-based localization approach for crowdsourced air traffic communication networks," *IEEE Transactions on Aerospace and Electronic Systems*, vol. 54, no. 3, pp. 1519–1529, 2018.

[8] S. Ayhan and H. Samet, "Aircraft trajectory prediction made easy with predictive analytics," in *KDD '16: Proceedings of the 22nd ACM SIGKDD International Conference on Knowledge Discovery and Data Mining*, 08 2016, pp. 21–30.

[9] Z. Xu, W. Zeng, X. Chu, and P. Cao, "Multi-aircraft trajectory collaborative prediction based on social long short-term memory network," *Aerospace*, vol. 8, no. 4, 2021. [Online]. Available: https://www.mdpi.com/2226-4310/8/4/115

[10] W. Zeng, Z. Quan, Z. Zhao, C. Xie, and X. Lu, "A deep learning approach for aircraft trajectory prediction in terminal airspace," *IEEE Access*, vol. 8, pp. 151 250–151 266, 2020.

[11] L. Xi, Z. Jun, Z. Yanbo, and L. Wei, "Simulation study of algorithms for aircraft trajectory prediction based on ads-b technology," in *2008 Asia Simulation Conference - 7th International Conference on System Simulation and Scientific Computing*, 2008, pp. 322–327.

[12] Y. Jing, J. Xu, G. M. Dimirovski, and Y. Zhou, "Optimal nonlinear estimation for aircraft flight control in wind shear," in *2009 American Control Conference*, 2009, pp. 3813–3818.

[13] J. BAUER and D. ANDRISANI, "Estimating short-period dynamics using an extended kalman filter," in *Orbital Debris Conference: Technical Issues andFuture Directions*, 1990. [Online]. Available: https://arc.aiaa.org/doi/abs/10.2514/6.1990-1277

[14] A. Weinert, N. Underhill, B. Gill, and A. Wicks, "Processing of Crowdsourced Observations of Aircraft in a High Performance Computing Environment," in *2020 IEEE High Performance Extreme Computing Conference (HPEC)*. IEEE, Sep. 2020, pp. 1–6.

APPENDIX

A. Extended Kalman Filter (EKF) Equations

Both implemented versions follow the traditional predict-update step of the EKF filter, as shown below:

Predict Step:

$$\mu_{t+1|t} = f(\mu_{t|t})$$
$$\Sigma_{t+1|t} = A_t \Sigma_{t|t} A_t^T + Q$$

Update Step:

$$\mu_{t|t} = \mu_{t|t-1} + K_t \left(y_t - g(\mu_{t|t-1})\right)$$
$$\Sigma_{t|t} = \Sigma_{t|t-1} - K_t C_t \Sigma_{t|t-1}$$
$$\text{where } K_t = \Sigma_{t|t-1} C_t^T \left(C_t \Sigma_{t|t-1} C_t^T + R\right)^{-1}$$

B. Method 1 Jacobian Matrices

$$A_t = \begin{bmatrix} I_{3x3} & \begin{bmatrix} (\Delta t + \beta_t) sin\,\theta_t & (\Delta t + \beta_t) v_t \cos\theta_t & 0 \\ (\Delta t + \beta_t) \cos\theta_t & -(\Delta t + \beta_t) v_t \sin\theta_t & 0 \\ 0 & 0 & \Delta t + \beta_t \end{bmatrix} & O_{3x1} & \begin{bmatrix} v_t \sin\theta_t \\ v_t \cos\theta_t \\ \dot{z}_t \end{bmatrix} \\ O_{5x3} & \begin{matrix} I_{3x3} \\ O_{2x3} \end{matrix} & O_{5x1} & O_{5x1} \end{bmatrix}$$

$$C_t = \begin{bmatrix} I_{6x6} & \begin{bmatrix} O_{5x1} \\ 1 \end{bmatrix} & O_{6x1} \end{bmatrix}$$

C. Method 2 Jacobian Matrices

$$A_t = \begin{bmatrix} I_{5x5} & O_{5x1} & \begin{bmatrix} u(t)_v \sin u(t)_\theta \\ u(t)_\theta \cos u(t)_\theta \\ u(t)_{\dot{z}} \\ O_{2x1} \end{bmatrix} \end{bmatrix}$$

$$C_t = \begin{bmatrix} I_{3x3} & \begin{bmatrix} O_{2x1} \\ 1 \end{bmatrix} & O_{3x1} \end{bmatrix}$$